

# Inelastic-neutron-scattering study of antiferromagnetic fluctuations in $\text{YBa}_2\text{Cu}_3\text{O}_{6.97}$

P. Bourges

*Laboratoire Léon Brillouin, CEA-CNRS, Centre d'Etudes de Saclay, 91191 Gif-sur-Yvette, France*

L. P. Regnault

*Centre d'Etudes Nucléaires de Grenoble, Département de Recherche Fondamentale sur la Matière Condensée, Service de Physique Statistique, Magnétisme et Supraconductivité, Groupe Magnétisme et diffraction Neutronique, Boîte Postale No. 85 X, 38041 Grenoble Cedex, France*

Y. Sidis

*Laboratoire Léon Brillouin, CEA-CNRS, Centre d'Etudes de Saclay, 91191 Gif-sur-Yvette, France*

C. Vettier

*European Synchrotron Research Facility, Boîte Postale No. 220, 38043 Grenoble Cedex, France*

(Received 10 November 1994; revised manuscript received 1 August 1995)

Inelastic-neutron-scattering experiments have been performed to study the spin-excitation spectrum in the overdoped regime of the high- $T_c$  superconducting system  $\text{YBa}_2\text{Cu}_3\text{O}_{6+x}$ ,  $x=0.97$ . All the observed magnetic fluctuations are peaked at the antiferromagnetic wave vector. In the superconducting state, the magnetic response is restricted over a limited energy range ( $\hbar\omega=33\text{--}46$  meV). The imaginary part of the magnetic susceptibility is characterized by two contributions defined by different  $q$  widths and different temperature dependences. A resonant contribution, which displays a narrower  $q$  width, appears to be connected with superconductivity. The two contributions can be accounted for in the framework of the  $t\text{-}t'\text{-}J$  model in the presence of superconductivity. The main new feature in the overdoped regime is the partial disappearance of magnetic correlations for temperatures above the superconducting temperature.

## I. INTRODUCTION

The persistence of antiferromagnetic (AF) fluctuations in the superconducting state of high- $T_c$  cuprates is one of the most striking features in these materials. The knowledge of the wave-vector and energy dependences of the imaginary part of the magnetic susceptibility,  $\chi''(\vec{Q}, \hbar\omega)$ , is of the most importance when building up an appropriate theory for high- $T_c$  superconductivity. With the availability of sufficiently large single crystals, a considerable amount of inelastic-neutron-scattering (INS) experiments have been performed<sup>1-4</sup> in order to characterize the dynamical magnetic correlations in all typical regimes of the cuprate phase diagram. Magnetic fluctuations are observed to be either commensurate peaked at AF wave vector  $\vec{Q}_{\text{AF}}=(\pi, \pi)$  in the  $\text{YBa}_2\text{Cu}_3\text{O}_{6+x}$  (YBCO) system<sup>1-3</sup> or incommensurate away from  $\vec{Q}_{\text{AF}}$  in the  $\text{La}_{2-x}\text{Sr}_x\text{CuO}_4$  (LSCO) system.<sup>4</sup> However, assuming that magnetism probed by INS experiments is correlated with the charge carriers, these apparently conflicting INS results reflect the difference in the Fermi surface (FS) topology.<sup>5</sup> The Fermi surface in YBCO, which has been observed using angle-resolved photoemission spectroscopy technique,<sup>6</sup> is clearly different from the usual FS shape which is expected from the simple tight-binding model for single  $\text{CuO}_2$  layer system like LSCO.

In the metallic state of  $\text{YBa}_2\text{Cu}_3\text{O}_{6+x}$  system, INS has established the existence of an *energy gap* in the imaginary part of the spin susceptibility (spin gap) (see Ref. 1 for a complete review): at low temperature, no intensity can be found below some characteristic energy,  $E_G$ . In the heavily

doped regime ( $0.65 \leq x \leq 0.94$ ), this spin-gap energy is related to  $T_c$  as  $E_G \approx 3.4 k_B T_c$ . In the weakly-doped regime ( $T_c \leq 55$  K or  $0.4 < x \leq 0.65$ ),  $E_G$  is much smaller and is sensitive to small variations in  $T_c$ : a change in  $T_c$  from 45 to 51 K leads to a change in  $E_G$  from 2.5 to 5 meV. As these two samples have nearly the same oxygen content, the change in  $E_G$  can be understood as a result of a specific ordering of oxygen in  $\text{Cu-O}$  chains (i.e., related to the real number of holes transferred in  $\text{CuO}_2$  planes). Note that superconducting samples with good homogeneity (sharp transition at  $T_c$ ) always exhibit a clear gap in the magnetic response.

The temperature dependence,  $E_G(T)$ , is not fully established: when increasing temperature, there is no sign that  $E_G$  decreases. However, magnetic scattering appears below  $E_G(T=0)$  upon raising the temperature, filling the gap completely at a temperature  $T_{\text{INS}}^*$  always larger than  $T_c$ .<sup>1,7,10</sup> This point has been interpreted as resulting from the opening of a *pseudogap* in the spin-excitation spectrum at  $T_{\text{INS}}^*$  because the weight of low-energy AF fluctuations starts to recede at  $T_{\text{INS}}^*$  with decreasing temperature. It is important to notice that the pseudogap behavior of the spin-excitation spectrum does not preclude any temperature dependence of the spin gap  $E_G(T)$ .

Furthermore, <sup>63</sup>Cu nuclear magnetic-resonance (NMR) studies<sup>8</sup> have revealed that the relaxation rate does not follow a Korringa law, as a consequence of AF fluctuations at the copper site. Actually,  $1/T_1 T$  exhibits a maximum at a temperature  $T_{\text{NMR}}^*$  which is larger than  $T_c$  in underdoped regime ( $x \leq 0.94$ ) whereas in overdoped regime ( $0.94 < x \leq 1$ ),  $T_{\text{NMR}}^*$

almost coincides with the superconducting transition. Thus, this behavior also reveals the existence of the pseudogap in the spin dynamics but only in the underdoped state. Therefore, both techniques suggest that there exists a pseudogap effect in the spin-excitation spectrum in the heavily doped regime at a temperature which appears to be the same in both experiments ( $T_{\text{NMR}}^* \approx T_{\text{INS}}^*$ , see Horvatic *et al.*<sup>8</sup>). However, the question whether or not these temperatures also coincide in the weakly doped regime remains unclear.

In the superconducting state, INS experiments have also shown that  $\chi''(q_{\text{AF}}, \hbar\omega)$  is characterized by a strong enhancement of the intensity at some energy  $E_r$ , observed at  $E_r = 41$  meV in  $x = 0.92$  sample.<sup>7</sup> As this enhancement is almost energy resolution limited, it looks like a *resonance* feature and exhibits a narrower  $q$  width than the magnetic response at other energies. Moreover, this resonance might be relevant to superconductivity since it abruptly vanishes at the superconducting transition, in contrast with the other part of the magnetic susceptibility. Its intensity decreases on increasing temperature, but  $E_r$  remains located at the same energy. Due to the filling of the spin gap upon increasing temperature, the temperature dependence of the total spectrum resembles a transfer of intensity from around  $E_r$  to below the spin gap.<sup>7</sup>

In the overdoped regime, controversies exist in the literature concerning the existence of the spin gap and the shape of  $\chi''$ . On the one hand, Rossat-Mignod *et al.*<sup>9</sup> have reported on the existence of a spin gap in YBCO<sub>7</sub> at  $E_G = 26$  meV and a resonance peak around  $E_r \approx 40$  meV. The thermal behavior was mainly analogous to that measured in the underdoped regime, except that no pseudogap was observed. Magnetic fluctuations at low energy are restored and  $\chi''$  passes through a maximum at  $T_c$ . On the other hand, Mook *et al.*,<sup>2</sup> using polarized neutrons, claimed that the spin-excitation spectrum consists only of an excitation at 41 meV which is strongly temperature-dependent superimposed on a weak constant continuum which is measured at all energies. These two conflicting results have at least one common characteristic: it is established that magnetic excitations are found at low temperature around 40 meV, and this peak exhibits a clear change in intensity at  $T_c$ .

In order to check carefully some key points in the behavior of  $\chi''(\vec{Q}, \hbar\omega)$ , we have performed unpolarized INS experiments on a different YBCO sample in the overdoped state,  $x = 0.97$ . Our results appear to be similar to our previous measurements but with important quantitative corrections. Basically,  $\chi''$  is found to be characterized in the superconducting state by a strong peak around 39 meV which occurs above a spin gap located at 33 meV. The main result is that correlated magnetism has almost vanished above  $T_c$ . One has to underline that this leads to a quite different picture as compared to underdoped samples<sup>7,10</sup> where AF correlations remain observable well above  $T_c$ .

The paper is organized as follows: in the next section, the INS experiment is presented. In Sec. III, we first discuss how the magnetic susceptibility is extracted from neutron intensities and we then present the characteristics of  $\chi''$  (existence of the spin gap, high-energy cutoff, wave vector, and temperature dependences), as measured by INS in the metallic overdoped regime of YBCO. In the last section, a comparison is made between theoretical predictions for the energy profile of the imaginary part of the magnetic susceptibility.

## II. EXPERIMENTS

### A. Neutron scattering

INS experiments provide the energy and the momentum dependences of the imaginary part of the dynamical magnetic susceptibility. In terms of  $\chi''(\vec{Q}, \hbar\omega)$ , the magnetic cross section can be expressed via the detailed balance

$$\frac{d^2\sigma}{d\Omega d\hbar\omega} \propto f^2(Q) |F(Q)|^2 \frac{1}{1 - \exp(-\hbar\omega/k_B T)} \chi''(\vec{Q}, \hbar\omega), \quad (1)$$

where  $f(Q)$  is the magnetic form factor for a  $\text{Cu}^{2+}$  atom and  $F(Q)$  is the inelastic structure factor. In the metallic state of YBCO, the wave-vector dependence of  $\chi''$  is usually found almost independent of the energy transfer (after resolution corrections).<sup>1,10</sup> Here, a noticeable change of the  $q$  shape versus  $\hbar\omega$  is observed around the resonance energy. Nevertheless, we still assume to split into two terms the  $q$  dependence of  $\chi''$  from its  $\hbar\omega$  dependence. Thus, since  $\chi''(\vec{Q}, \hbar\omega)$  can be parametrized by a simple Gaussian line in the (110) direction of  $q$  space,<sup>1,3</sup> it can be written as

$$\chi''(\vec{Q}, \hbar\omega) = \chi''(\vec{Q}_{\text{AF}}, \hbar\omega) \exp\left[-4 \ln^2\left(\frac{q - q_{\text{AF}}}{\Delta_q}\right)^2\right], \quad (2)$$

where  $q_{\text{AF}} = 1/2$  and  $\Delta_q$  is the full width at half maximum (FWHM) of the magnetic intensity at fixed energy transfer. Actually, the measured intensity is the convolution product of the above cross section (1) with the spectrometer resolution function. Because, the triple-axis resolution function is generally assumed to have a Gaussian shape in both  $\omega$  and  $q$  spaces, the parametrization form (2) has the advantage of being analytically deconvolved.<sup>3</sup> However, a squared Lorentzian, which is generally used in two-dimensional magnetic system, can fit the  $q$  scan as well.<sup>10</sup> Actually, as there is no clear physical reason to choose one shape or the other, we have used the Gaussian line (2) for the sake of simplicity.

INS experiments were carried out on the 2 T triple-axis spectrometer installed on a thermal beam located at the Orphée reactor in Saclay. Pyrolytic graphite (PG002) as well as copper (Cu111) crystals have been used as monochromators and a PG002 crystal as analyzer. In order to increase the neutron flux at the sample position, monochromators and analyzer focus the neutron beam horizontally and vertically. Curvatures are fixed and optimized for an average value of commonly used incident and final wave vectors. A detailed description of such improvements on this spectrometer has been recently emphasized.<sup>11</sup> PG filters are employed to suppress higher-order contamination in the diffracted beam with fixed final energy  $E_f = 35$  meV ( $k_f = 4.1 \text{ \AA}^{-1}$ ). No correction for higher-order contamination in the monitor has been performed as is usually the case when working in such a wave-vector range on thermal beam. On the other hand, due to the curvatures of the monochromator, a correction of the data should be, in principle, made as a consequence of the change of the focal point when moving the incident energy. This effect, which is partly taken into account by the monitor, requires a correction which is negligible here due to the small energy window of interest 30–45 meV. No collimators were used, yielding an energy resolution width which is

equivalent to that of a conventional spectrometer with 40/40/40/40 collimations. Typical resolution FWHM values are  $\Delta\omega = 4.7$  meV,  $\Delta q = 0.1 \text{ \AA}^{-1}$  for a longitudinal scan using Cu111 monochromator for a final wave vector  $k_f = 4.1 \text{ \AA}^{-1}$ , an energy transfer of  $\hbar\omega = 30$  meV and a wave vector  $Q = 3 \text{ \AA}^{-1}$ .

### B. Sample characterization

The YBCO<sub>7</sub> single crystal, which has also been used in previous phonon measurements,<sup>12</sup> has been grown by a zone-melting method by the Hoechst Company. An ac-susceptibility measurement<sup>12</sup> revealed an onset superconducting transition at  $T_c = 92.5$  K with a sharp transition width of less than 1 K. The orthorhombicity, expressed as  $200(b-a)/(b+a) = 0.168(5)$ , is in agreement with powder-diffraction measurements<sup>13</sup> for fully oxidized samples. This as-grown crystal belongs to the overdoped regime as  $T_c$  is reduced from 94 K.<sup>14</sup> The lattice constants, determined at room temperature, were  $a = 3.822(2) \text{ \AA}$ ,  $b = 3.886(2) \text{ \AA}$ , and  $c = 11.678(5) \text{ \AA}$ . By comparison with powder-diffraction data,<sup>13</sup> the oxygen content may be estimated at  $x = 0.97 \pm 0.02$ .

The sample has the shape of a half cylinder with a  $0.6 \text{ cm}^3$  volume. It is mainly composed of two grains misoriented by about  $2^\circ$ . The two parts exhibit almost the same mosaic spread ( $\approx 1.5^\circ$ ). Since the spin fluctuations are weakly correlated (typically one or two unit cells in this overdoped state), this crystalline defect as well as the orthorhombicity do not affect our measurements. The sample was clamped to an Al grid and attached to the cold finger of an ILL-type cryostat. It was mounted with (110) and (001) directions within the horizontal scattering plane. The temperature was measured and controlled by a carbon or a platinum sensor depending on the temperature range.

## III. DYNAMICAL MAGNETIC SUSCEPTIBILITY

### A. How the magnetic intensity is extracted

For an oxygen content larger than  $x = 0.8$ , magnetic scattering in the superconducting state of YBCO has been found above the spin gap,  $E_G$ , located above 25 meV. Thus, we have focused our investigation on a restricted energy window between 25 and 50 meV where magnetic intensity is expected to dominate from prior investigations.<sup>1,7,9,10</sup> Besides, YBCO has a CuO<sub>2</sub>-bilayer structure, and only in-phase ‘‘acoustic’’ magnetic structure factor has been observed so far. This AF structure factor exhibits maxima along the AF rod  $Q_{AF} = (1/2, 1/2, q_1)$  at  $q_1 \approx 1.6$  and  $q_1 \approx 5.2$ . Then, to explore the energy range of interest, scattering kinematics make it necessary to move out around  $q_1 \approx 5.2$ . Unfortunately, as it has been stressed in previous studies of magnetic fluctuations in the YBCO system,<sup>1,7</sup> energy scans performed at the AF wave vector  $Q_{AF} = (0.5, 0.5, 5.2)$  reveal a quite complex line shape whereas nuclear contributions constitute the main part of the neutron signal. Especially, around 20 meV, large nuclear contributions occur<sup>1,7,10</sup> which prevent an accurate determination of the magnetic scattering around this energy when the AF correlations are not strong enough. The main experimental difficulty is then to extract the magnetic intensity from these nuclear contributions. Several arguments are used to address this point:

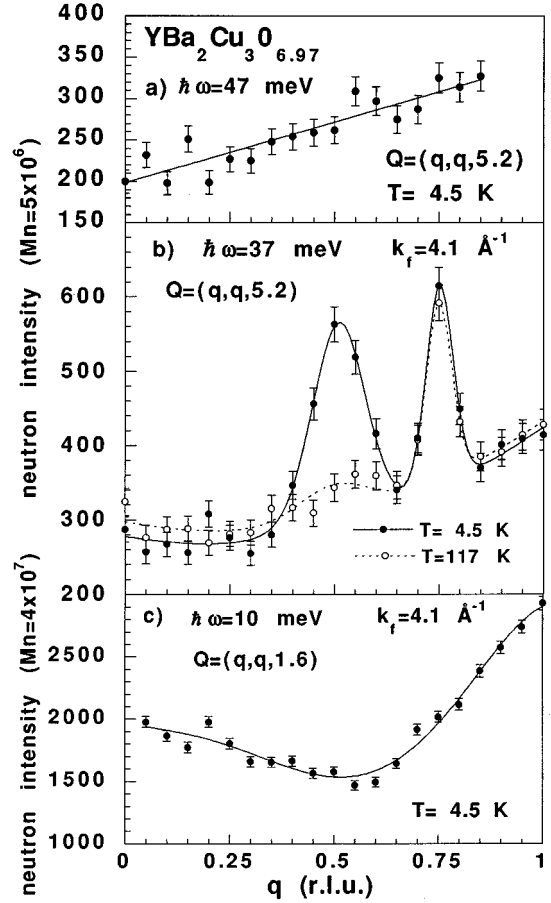


FIG. 1.  $Q$  scans across the magnetic rod at fixed energy transfers: (a)  $\hbar\omega = 47$  meV at  $T = 4.5$  K. (b)  $\hbar\omega = 37$  meV at  $T = 4.5$  K (closed circles) and  $T = 117$  K (open circles). The contribution peaked at  $q = 0.75$  is a usual spurious peak due to some incoherent process on the Cu111 monochromator (For instance, see Ref. 3). (c)  $\hbar\omega = 10$  meV at  $T = 4.5$  K. The lines are fits as explained in the text.

(i) Performing  $q$  scans across the magnetic rod at fixed energy transfer allows to separate flat contributions from correlated intensity peaked at  $Q_{AF}$ . Figures 1(a)–1(c) depict such  $q$  scans in the (110) direction performed at energy transfers  $\hbar\omega = 47$ , 37, and 10 meV, respectively. At  $\hbar\omega = 10$  and 47 meV, no peak at  $q = 0.5$  is seen in these scans meaning no magnetic correlations at these energies.

(ii) Similarly to Figs. 1(a) and 1(c), the scan at  $\hbar\omega = 37$  meV at  $T = 117$  K [Fig. 1(b)] indicates very small intensity peaked at  $q = 0.5$  in contrast with the same measurement performed at 4.5 K where an intense component obviously exists at  $Q_{AF}$ . This new feature has important consequences and indicates a rapid decrease of AF correlations upon heating. Indeed, the temperature dependence of any nuclear contribution is only expected to obey the following standard temperature factor,  $[1 - \exp(-\hbar\omega/k_B T)]^{-1}$ . In the energy range of interest, this factor is unity for temperature smaller than 117 K ( $\approx 10$  meV). Then, all the part of the neutron intensity which changes with temperature below  $T = 117$  K corresponds to magnetic fluctuations.

(iii) Furthermore,  $q$  scans performed at higher temperatures ( $T = 150$  and  $190$  K), at  $\hbar\omega = 37$  meV (or at  $\hbar\omega = 39$  meV) show no change from what is measured at  $T = 117$  K

indicating that no correlated magnetic signal does exist above  $T=117$  K, or at least is too small to be observed. Minute magnetic contributions may indeed exist ( $\leq 20$  counts) within the error bars at  $T=117$  K [see Fig. 1(b)]. So, from these  $q$  scans at fixed energy transfer and their temperature dependence, one can distinguish the magnetic contribution from the background.

(iv) The next point is to obtain the background for all energies. As neutron intensities can be found peaked at  $\vec{Q}_{AF}$  which are not related to magnetic fluctuations, the simple wave-vector-dependence argument cannot be used for all energies. Then to solve this problem, we use the fact that the magnetic response in the previous measurements has always been found to be quite monotonic as a function of energy above  $T=100$  K for all oxygen contents. Therefore, the neutron intensity which is peaked at the AF wave vector and which persists at  $T=117$  K in this overdoped regime cannot be of magnetic origin.

(v) Thus, using the above arguments, we will use the energy scan obtained at  $T=117$  K [Fig. 2(a)] as the nuclear contribution or background to determine the correlated magnetic contribution. Then, the imaginary part of the magnetic susceptibility [Figs. 2(b) and 6] has been obtained by taking differences between energy scans measured below  $T=100$  K and the energy scan measured at  $T=117$  K. This method to separate the magnetic part from the nuclear part may only underestimate AF fluctuations. Also, it has to be stressed that such a procedure of background subtraction may give limitations about the  $\chi''$  shape in case of very weak magnetic signal.

The above discussion implies some comments about (i) the energy shape of the “background” and (ii) the previous results. The energy scan performed at  $T=117$  K, shown in Fig. 2(a), indicates the presence of two peaks at 30.5 and 42.5 meV in addition to the large smooth nuclear contribution spread over the whole spectral range. From what has been said above, we conclude that these two peaks correspond to phonon contributions. Their  $q$  width would then be related to their dispersion from the two sides of Brillouin-zone boundary in (110) direction. However, as phonons are actually found to be almost dispersionless in this frequency range,<sup>12</sup> phonons do not seem to account for the  $q$  dependence of these two peaks. However, as recently pointed out by Fong *et al.*,<sup>15</sup> the peak at 42.5 meV is reliably related with a dispersionless phonon mode but with a  $q$ -dependent structure factor yielding an apparent  $q$  width in agreement with the measurements. Here, being mainly interested in the magnetic response, we consider these contributions as part of the nuclear background. The upper nuclear peak at 42.5 meV was already observed and taken into account in our previous YBCO<sub>7</sub> study<sup>1,9</sup> but the contribution at 30.5 meV had been previously incorrectly incorporated as magnetic correlations. This had led to (i) a smaller spin gap and (ii) a larger  $q$  width  $\Delta q=0.3$  r.l.u. Actually, this contribution at 30 meV does not change with temperature [see Fig. 2(a)] in contrast to the magnetic part. This last nuclear contribution exists at all oxygen contents and therefore it implies corrections on the determination of magnetic contribution for all oxygen contents. Fortunately, in the case of lower doping, the magnetic response is stronger and such a correction does not affect our

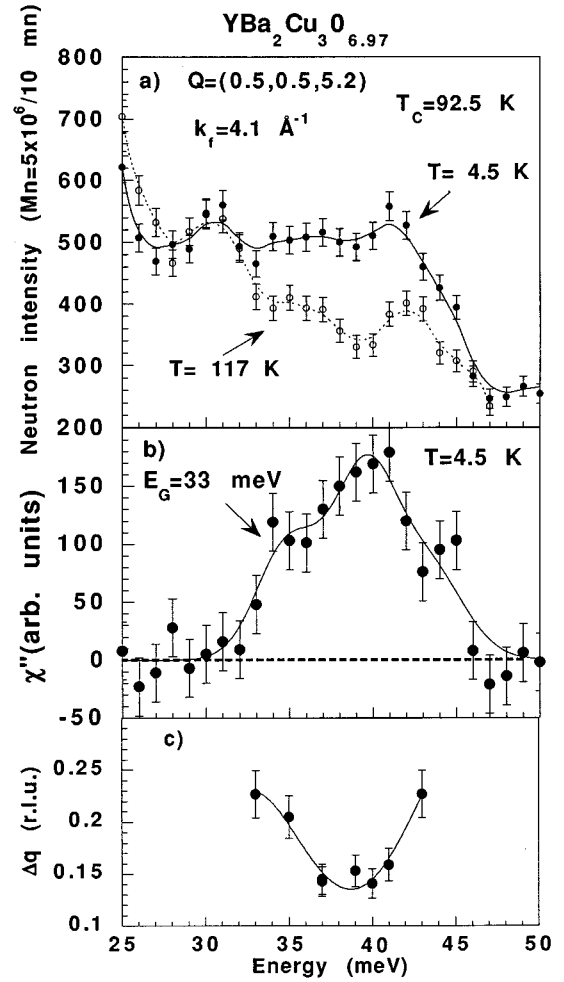


FIG. 2. (a) Energy-scans at  $(\pi, \pi)$  position at  $T=4.5$  and 117 K obtained with the Cu111 monochromator. The increase in intensity of the lower energy part ( $\hbar\omega=25-27$  meV) is only due to a broadening with increasing temperature of the nuclear contribution centered at  $\hbar\omega=21.5$  meV (see Ref. 1). (b)  $\chi''(q_{AF}, \hbar\omega)$  obtained from the difference from the energy scan at  $T=4.5$  and 117 K (see text). (c) FWHM  $q$  width in (110) direction obtained either from the difference of  $q$  scans at  $T=4.5$  and 117 K or from scans at  $T=4.5$  K at an energy free from nuclear contributions. The resolution  $q$  width is quite constant in this  $\omega$  range ( $\Delta q=0.1$  r.l.u.). The lines are guides for the eye.

final conclusions. For instance, in our YBCO<sub>6.92</sub> study, the clear temperature dependence at 30 meV indicates that AF correlations do exist at this energy for this oxygen concentration.<sup>7,10</sup> Similar analysis has been performed recently by Fong *et al.*<sup>15</sup> to get the magnetic scattering at the wave vector  $\vec{Q}=(1.5,0.5,1.7)$  where the phonon peak at 42.5 meV is much weaker but the peak around 30.5 meV still exists.

In the following, we will analyze and discuss the magnetic response as determined from the above-mentioned method. We will consider successively the energy, wave-vector, and temperature dependences of  $\chi''(\vec{Q}_{AF}, \hbar\omega)$ .

### B. Energy dependence of $\chi''(\vec{Q}_{AF}, \hbar\omega)$

Figure 2(b) shows  $\chi''(\vec{Q}_{AF}, \hbar\omega)$  obtained at  $T=4.5$  K, located well below  $T_c$ . Quite surprisingly, the magnetic re-

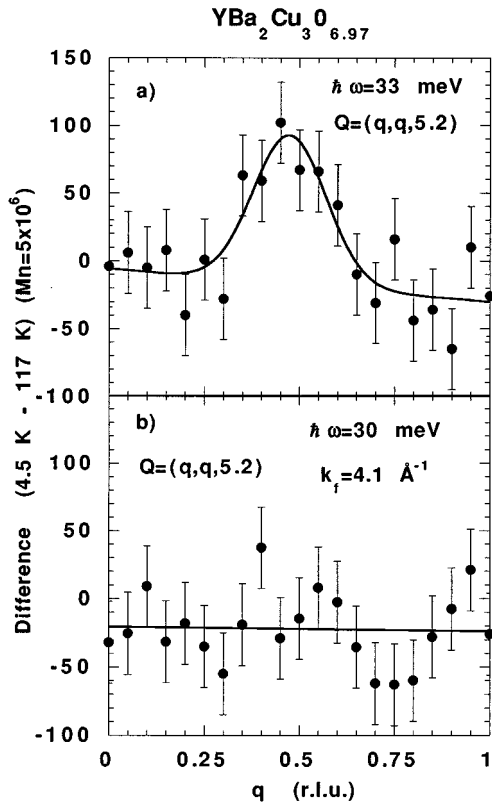


FIG. 3. Difference between  $q$  scans in (110) direction obtained at  $T=4.5$  and at 117 K for two fixed energy transfers  $\hbar\omega=30$  and 33 meV. The lines are fit to a Gaussian function as given by Eq. (2).

response is restricted to a small range in energy between 32 and 46 meV. It has to be stressed that this energy range is larger than the resolution energy width,  $\Delta\omega^{\text{res}}=4.7$  meV.  $\chi''$  displays a well-defined maximum at  $\hbar\omega=39$  meV and a shoulder around 35 meV. These two features will be discussed later when considering the  $Q$ , and  $T$  dependences of  $\chi''$ . Nevertheless, let us stress here that the peak at 39 meV, is called the *resonance* and corresponds to the major feature of the spin dynamics in this overdoped regime. It has been reported around 40 meV in all INS measurements<sup>1,2,7,9,10,15</sup> for  $x>0.9$ .

The magnetic response is limited on the small energy side by a *spin gap* at  $E_G=33\pm 1$  meV which is defined as previously<sup>1,7</sup> by the inflexion point in  $\chi''(\omega)$  curve (to account for the  $\omega$  width of the resolution). The lack of signal below 31 meV is unambiguously demonstrated by a comparison of differences between  $q$  scans at  $T=4.5$  and 117 K, for energies located below and above the gap. Figure 3 shows such differences for two energy transfers  $\hbar\omega=30$  and 33 meV. Clearly, a signal peaked at  $Q_{\text{AF}}$  with a FWHM  $\Delta q=0.23\pm 0.02$  r.l.u. is observed at 33 meV whereas nothing is visible at 30 meV.

In agreement with our previous YBCO<sub>7</sub> investigation,<sup>9</sup>  $\chi''$  is also strongly depressed on the high-energy side defining a “*cutoff*” energy,  $E_c=46$  meV. This fact is illustrated from a  $q$  scan performed at  $\hbar\omega=47$  meV [see Fig. 1(a)] which shows no trace of a correlated signal around  $q_{\text{AF}}=0.5$ . However, in underdoped states  $x=0.92$  (Ref. 7) and  $x=0.83$ ,<sup>16</sup> an AF response has been observed at an energy transfer as high as  $\hbar\omega=50$  meV but with a smaller magnitude than at lower

energy. Therefore, this cutoff effect is enhanced in the overdoped regime, strongly reducing the energy range where AF correlations do exist. We will show later that such an effect corresponds to the vanishing of one type of magnetic fluctuations when going from the underdoped regime to the overdoped regime.

Performing the same treatment on our previous YBCO<sub>7</sub> data,<sup>1,9</sup> for which the energy scan performed at  $T=150$  K has been taken as the background, yields an imaginary part of the dynamical susceptibility with a spin gap ( $E_G=32$  meV) and a cutoff ( $E_c=43$  meV).<sup>10</sup> In the stoichiometric sample  $x=1$ , the magnetic correlations appear over a more restricted energy range than in the  $x=0.97$  sample as a consequence of being more overdoped (i.e., the number of holes in the CuO<sub>2</sub> planes continues to increase). However, in our previous YBCO<sub>7</sub> sample,  $T_c$  was found to be 89 K due to an addition of 3.5% of Sr impurities at the Ba site leading to a small reduction of  $T_c$  by a couple of degrees. Then, the slight reduction of the energy of the AF fluctuations (i.e., roughly the energy of the resonance peak  $\hbar\omega\approx 38$  meV) may be linked to the small reduction in  $T_c$ . Obviously, the same reasoning applies to the reduction of the spin-gap value.

All neutron measurements confirm the absence of a sizable AF signal at energies below the spin gap at low temperature. Figure 1(c) shows a  $q$  scan performed at an energy  $\hbar\omega=10$  meV at a temperature  $T=4.5$  K ( $T/T_c\approx 0.05$ ) and with a monitor count eight times larger than the measurements at higher energy. Within the error bars, *no* peaked signal could be detected, indicating that either the magnetic response is uncorrelated, or that it is very weak. Consequently, INS experiments would agree that a spin gap opens also in the overdoped regime in the range 32–35 meV. For instance, assuming that the continuum intensity reported in the superconducting state by Mook *et al.*<sup>2</sup> is either uncorrelated or nonphysical, one may estimate a spin gap at  $E_G=35\pm 2$  meV from their measurements for a sample with an oxygen content close to our sample as deduced from the  $T_c$  value ( $T_c=92.4$  K) and the lattice constants. But, in contrast with our previous conclusion,<sup>1,9</sup> the spin gap continues to increase with doping going from the underdoped regime to the overdoped region of the phase diagram.

### C. Wave-vector dependence of $\chi''(Q, \hbar\omega)$

The  $q$  scans in (110) direction, either directly measured at low temperature or from the difference of  $q$  scans obtained at different temperatures (for energies where “phonon” contribution exists), have been analyzed in terms of a Gaussian functional form. From a best fit to Eq. (2), one may deduce the  $q$  width (FWHM)  $\Delta q$  as a function of energy. The resulting dependence  $\Delta q(\omega)$  is reported in Fig. 2(c).  $\Delta q$  displays a well pronounced minimum around  $39\pm 2$  meV. Between  $\hbar\omega=37$  and 41 meV, the FWHM is almost constant, with a value  $\Delta q=0.14\pm 0.01$  r.l.u., which gives after a simple Gaussian deconvolution  $\Delta q=0.23 \text{ \AA}^{-1}$  (FWHM) whereas one has  $\Delta q=0.22\pm 0.02$  r.l.u. away from this energy range, leading to  $\Delta q=0.45 \text{ \AA}^{-1}$  (FWHM) after Gaussian deconvolution. The narrowing of the spectrum in  $q$  space reveals the existence of the *resonance* feature at  $E_r=39$  meV [Fig. 2(b)], in an energy range which is almost controlled by the energy-resolution width. This resonance feature has been observed at a slightly larger value  $E_r=41$  meV in YBCO<sub>6.92</sub>,<sup>7</sup> but with

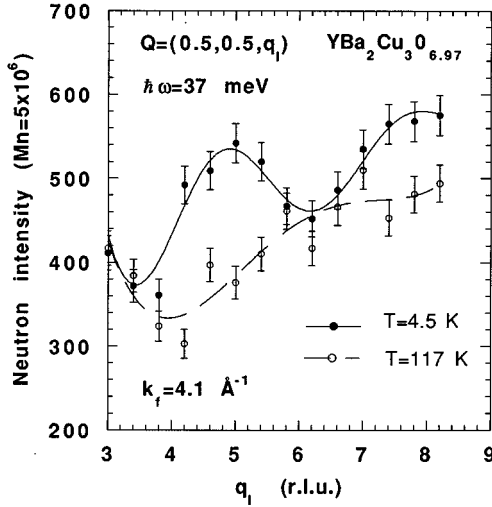


FIG. 4.  $Q_1$  scans along the magnetic rod for fixed energy transfer  $\hbar\omega=37$  meV at  $T=4.5$  K (closed circles) and at  $T=117$  K (open circles). The solid line is a fit by a magnetic “acoustic” modulation structure factor  $F(Q)^2$  (see text) times the  $\text{Cu}^{2+}$  form factor plus the background (dashed line) as measured at  $T=117$  K.

very similar characteristics. In addition to the resonance peak, a second contribution is detected over a broader energy range (between 32 and 46 meV), which is associated with an intrinsic  $q$  width twice as large. This latter contribution has also been observed in  $\text{YBCO}_{6.92}$ ,<sup>7,10</sup> however over a broader energy range (between 27 and 50 meV) and with a larger intensity (about a factor 2.5 after normalization<sup>10</sup>). An estimate of the associated intraplane AF correlation lengths can be obtained from the approximate relation  $\xi=2/\Delta q$ , which gives reduced values  $\xi/a=2.2\pm 0.2$  and  $\xi/a=1.1\pm 0.1$  for the resonant and nonresonant parts of  $\chi''$ , respectively.

Another interesting feature of YBCO is the existence of a strong AF coupling between spins in adjacent layers as a result of the bilayer structure of  $\text{CuO}_2$  planes in YBCO.<sup>1-3</sup> The magnetic inelastic structure factor in the metallic state of YBCO in Eq. (1) follows the acoustic modulation of magnons in the AF state:  $F(Q)=2 \sin(\pi z q_1)$ , where  $z c=3.38 \text{ \AA}$  is the distance between  $\text{Cu}(2)$  atoms located in adjacent layers. A  $q_1$  scan in the (001) direction (i.e., along the magnetic rod) at low temperature and the same scan obtained at  $T=117$  K are shown in Fig. 4 at  $\hbar\omega=37$  meV. It indicates that no modulated intensity is measurable at  $T=117$  K. Again, taking the difference between these two scans demonstrates that the AF coupling between the two  $\text{Cu}(2)$  layers remains unaffected even in this overdoped regime. This picture is in sharp contrast with our previous study<sup>9</sup> of the overdoped regime where a weaker AF coupling between the two  $\text{Cu}(2)$  layers has been deduced. Actually, this result had been obtained from a  $q_1$  scan performed at  $\hbar\omega=30$  meV where it is now clear that the intensity is not magnetic in origin. Here, a full modulation along (001) direction of the magnetic scattering is indeed observed at all energies where AF correlations exist [i.e., for energies reported in Fig. 2(b)]. Furthermore, as the measured intensity at  $q_1\approx 3.3$  or 6.6 (which are nodes of the magnetic “acoustic” modulation) does not change with temperature, no weakening of the bilayer coupling can be invoked to explain (i) the sharp decrease of the

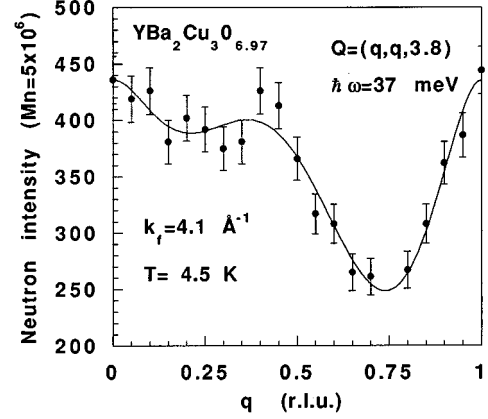


FIG. 5.  $Q$  scans across the magnetic rod at  $q_1=3.8$ ,  $\hbar\omega=37$  meV and  $T=4.5$  K. The line is a guide for the eye.

magnetic intensity on raising temperature, (ii) the decrease of magnetic scattering when going from the underdoped regime to the overdoped regime.<sup>10</sup> This last point is also documented by a  $q$  scan in the (110) direction performed at  $q_1=3.8$  and low temperature (see Fig. 5), which shows *no* correlated intensity around  $\bar{Q}_{\text{AF}}$  as a result of the magnetic “acoustic” modulation, very weak at this value of  $q_1$ .

#### D. Temperature dependence of $\chi''(\bar{Q}_{\text{AF}}, \hbar\omega)$

Figure 6 shows the temperature dependence of the imaginary part of the magnetic susceptibility measured at the antiferromagnetic point  $\bar{Q}_{\text{AF}}$ , for temperatures located both below and above  $T_c$ .  $\chi''(\bar{Q}_{\text{AF}}, \hbar\omega)$  in Fig. 6 has been obtained after subtraction at each temperature reported in the figure by the energy scan measured at  $T=117$  K. The data obtained below  $T_c$  exhibit a nonmonotonic temperature dependence when raising the temperature from 4.5 up to 95.6 K (i.e., slightly above  $T_c$ ). The peak at 40 meV associated with the resonance indeed decreases continuously whereas, for instance, the shoulder detected at 35 meV at low temperature seems to first increase on increasing temperature, passes through a maximum around 40 K and then decreases again. In other words, the shape of  $\chi''$  is not preserved when increasing the temperature. Therefore, it confirms the existence of *two different* contributions in the magnetic response because the temperature behavior of the resonance peak is markedly different from that at other energies. However, the data can be described by a single peak but with a less satisfactory fit. Therefore, due to the lack of statistics, new experiments should be achieved to completely ascertain this point.

Figure 7 displays the temperature dependence of the resonance peak intensity measured at an energy transfer  $\hbar\omega=40$  meV. In agreement with previous data by Rossat-Mignod *et al.*<sup>9</sup> and Mook *et al.*,<sup>2</sup> the resonance peak undergoes a clear change at  $T_c$ , above which temperature the scattering *remains constant* within the error bars, at least up to 190 K from our new data (see Fig. 8). Further information has been obtained from the temperature dependence of  $q$  scans performed at the same energy. We show in Fig. 8 typical results obtained at 4.5, 117, and 190 K, which all indicate peaked contributions at  $\bar{Q}_{\text{AF}}$  but with very different  $q$  widths:  $\Delta q$

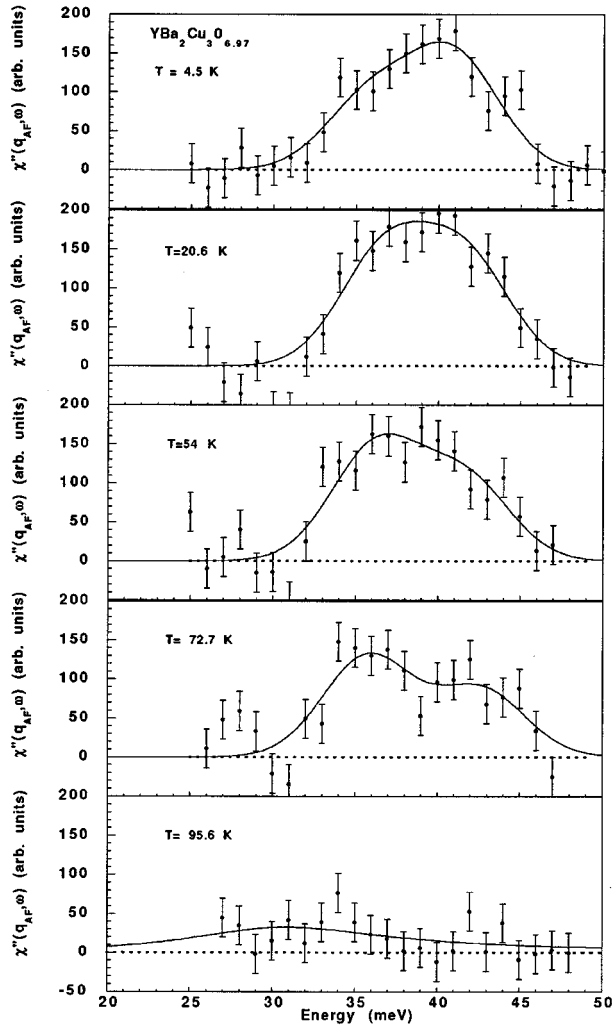


FIG. 6. Imaginary part of magnetic susceptibility at  $q_{AF}$  for different temperatures. It has been obtained from the difference between energy scans performed at different temperatures as indicated in the figure and the energy scan measured at  $T=117$  K [as shown in Fig. 2(a)]. The solid lines are guides for the eye.

$=0.19$  and  $0.24$  r.l.u., below  $T_c$  and above  $T_c$ , respectively. From the evolution of the intensities at  $T=117$  K as a function of wave vector and energy [see Fig. 1(b) and 2(a)], we have attributed this residual intensity above  $T_c$  as arising from the 42.5-meV-phonon peak previously identified in the beginning of this section. This could explain the very weak temperature dependencies observed above  $T_c$  (at least up to 190 K) in the various energy,  $q_1$ , and  $q$  scans. The same conclusion has been reached recently<sup>15</sup> by measuring the magnetic scattering at  $Q_{AF}=(1.5,0.5,1.7)$  where the 42.5 meV phonon peak is absent. Thus, the abrupt change in  $q$  width reported at  $\hbar\omega=41$  meV in Ref. 2 using *unpolarized* neutrons appears nonphysical, because the scattering detected above  $T_c$  (i.e., related to the larger  $\Delta q$ ) is dominated by a *nonmagnetic* contribution. Nevertheless, despite this difference in analysis, as far as  $q$  widths are concerned, our raw data appears in good quantitative agreement with those reported in Ref. 2. To the contrary, the FWHM  $q$  width obtained by Sato *et al.*<sup>17</sup> ( $\Delta q \approx 0.35$  r.l.u.) at  $\hbar\omega=36$  meV and  $T=10$  K in a YBCO<sub>6.90</sub> sample, is about two times larger than all other reports in this system for  $x>0.8$ . This is even

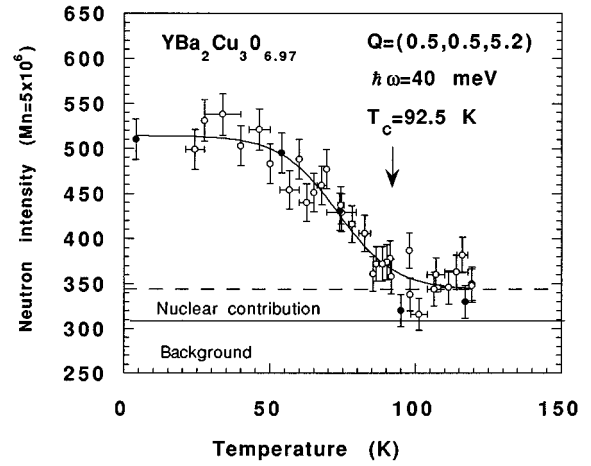


FIG. 7. Temperature dependence of the neutron intensity (open circles) at the AF wave vector near the resonance energy  $\hbar\omega=40$  meV and  $Q=(0.5,0.5,5.2)$ , closed circles are points from  $(q,q)$  scans. The line is a guide for the eye.

more surprising since the superconducting properties of their sample (e.g., the value of  $T_c$ ) are not very different from those observed in our sample.

The temperature dependence of  $\Delta q$  (Fig. 9) has been obtained after subtraction of the parasitic temperature-independent contribution. Within the experimental error bars,  $\Delta q$  appears constant below  $T_c$ . Unfortunately, as magnetic fluctuations are strongly reduced, no information could be obtained above  $T_c$ .

Due to its temperature dependence, one can conclude that this resonant contribution to  $\chi''(Q,\hbar\omega)$  observed only below  $T_c$ , is a *direct* manifestation of the opening of the superconducting gap. The second contribution to  $\chi''(Q,\hbar\omega)$  (i.e., the nonresonant part) is also enhanced by the presence of superconductivity, because it seems to vanish (or at least to become very small) above  $T \approx 100$  K as well. This is in sharp contrast to what has been observed in the normal state of underdoped YBCO.

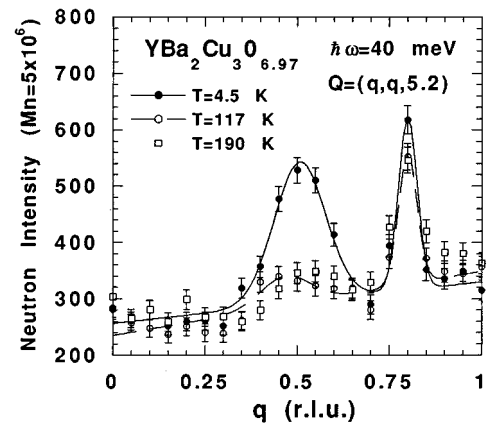


FIG. 8.  $Q$  scans across the magnetic rod at  $q_1=5.2$ ,  $\hbar\omega=40$  meV, and  $T=4.5$  K (closed circles) or  $T=117$  K (open circles). The contribution peaked at  $q=0.8$  is the same spurious peak as in Fig. 1(b). The lines are fits as explained in the text.

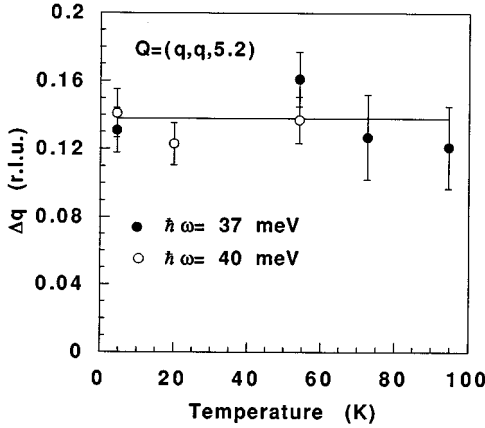


FIG. 9. Temperature dependence of FWHM  $q$  width in the (110) direction at  $\hbar\omega=37$  meV (closed circles) or at  $\hbar\omega=40$  meV (open circles).  $\Delta q$  has been deduced from differences from  $q$  scans at low temperature and  $T=117$  K for the latter energy.

Therefore, comparatively to the underdoped regime,<sup>10</sup> in the overdoped regime, the magnetic intensity above  $T_c$  is doubly reduced, first due to intrinsic decrease as  $x$  increases and second due to the more rapid decrease on increasing temperature. In our opinion, these two effects cannot be attributed to vanishing magnetic correlation lengths, neither in the  $\text{CuO}_2$  planes [as the intraplane  $q$  width does not exhibit any sizable change either with temperature or with doping for  $x \geq 0.8$  (Ref. 10)], nor between the  $\text{Cu}(2)$  layers (as the AF coupling is conserved in the overdoped regime).

From the above discussion, no magnetic intensity seems to occur in the normal state. However, as suggested at  $T=95.6$  K in Fig. 6, a weak magnetic contribution may remain above  $T_c$  with almost one order of magnitude less intensity. Due to its weakness, the determination of the energy dependence of this intensity is far outside the bounds of our data. However, they put limits on the amplitude of AF fluctuations in the normal state of the overdoped regime. Moreover, a low-energy study at  $\hbar\omega=10$  meV which emphasizes the temperature dependence of  $\chi''$  in the normal state confirms such a magnitude.<sup>18</sup> In any case, more accurate data have to be collected to clarify this point.

#### IV. DISCUSSION

To summarize, in the overdoped state of YBCO,  $\chi''(\vec{Q}, \hbar\omega)$  is characterized in the superconducting state by two dynamical contributions associated with two different  $q$  widths and restricted to a *narrow* energy range around 40 meV. However, these components cannot be separated in two independent parts. The whole spectrum displays a spin gap,  $E_G \approx 33$  meV, which is larger than in the underdoped regime. Both magnetic contributions rapidly decrease upon increasing the temperature with no sizable transfer of intensity to lower energies. In particular, the resonance feature vanishes at the superconducting transition temperature giving strong support that these magnetic fluctuations are intrinsically coupled to superconductivity. In the normal state, both contributions are replaced by a much weaker contribution which may exist over a broad energy range. However, the details of

this contribution (shape in energy, energy scales,...) could not be obtained from the present experiments. Such a weak magnetic scattering observed above  $T_c$  is different from what is measured in the underdoped regime<sup>7,10,16</sup> where intensity below the spin gap is easily observed above  $T_c$ .

To discuss the existing theories that propose a description of the spin dynamics in cuprates, we shall compare the energy and wave-vector *shapes* of  $\chi''(\vec{Q}, \hbar\omega)$ , as calculated following several approaches, with our experimental  $\chi''(\vec{Q}, \hbar\omega)$ . It is now accepted that a realistic model which can describe the magnetic properties of cuprates is the three band Hubbard model.<sup>19,20</sup> It can be developed in the limit of strong coupling when the Coulomb repulsion on copper site is larger than the hopping probability of holes associated with the copper site (so-called Zhang-Rice singlet<sup>21</sup>). In such a case, the Hubbard model is reduced to the so-called  $t$ - $J$  model or the  $t$ - $t'$ - $J$  model when next-nearest-neighbor hopping term is taking into account.<sup>20,22</sup> Depending on the approximation used to treat it, the  $t$ - $t'$ - $J$  model may account quite well for many aspects of the spin dynamics in both LSCO and YBCO systems.<sup>20</sup>

##### A. Existing theories for $\chi''(\vec{Q}, \hbar\omega)$

Let us consider the theoretical existence of the spin gap in the magnetic susceptibility,  $\chi''(\vec{Q}_{\text{AF}}, \hbar\omega)$ . Several theories can predict a spin gap, with a different origin depending on the model. In the framework of  $t$ - $t'$ - $J$  model using the slave-boson representation,<sup>22</sup> a gaplike behavior has been obtained for  $\chi''$  which is associated with the building of some singlet state resonating valence bond (RVB state). It is in contrast with the weak-coupling limit<sup>23</sup> or in the infinite  $U$  limit of the  $p$ - $d$  model<sup>5</sup> where the gap in  $\chi''$  exists due to the opening of the superconducting gap. However, in most of these approaches, the observed energy line shape of  $\chi''$  is badly reproduced because (i) a single contribution is generally expected above the energy gap, (ii) a tail in  $\chi''$  exists up to an energy of the order of the hopping parameter ( $t \approx 0.5$ – $2$  eV). Indeed, these models cannot explain the disappearance of magnetic intensity above some high-energy cutoff. In some of these theories, the wave-vector dependence of  $\chi''$  does not also correspond to the experimental one:  $\chi''$  is sometimes found not only maximum at the AF wave vector for the YBCO system.<sup>22,23</sup>

In contrast, *two magnetic contributions* to  $\chi''$  have been obtained with the  $t$ - $t'$ - $J$  model, but using a diagrammatic technique for the Hubbard operators.<sup>20</sup> The first one arises from the subsystem of itinerant charge carriers and is analogous to the magnetic susceptibility obtained in the weak-coupling approach.<sup>23</sup> The second one corresponds to the localized spin subsystem with short-range AF correlations associated with two-spinon spectral function. The key point is that both contributions are strongly coupled. Therefore, their interrelation may account for many features of the spin dynamics in YBCO.

In this approach, the gap in  $\chi''$  results from the opening of the superconducting gap whereas the pseudogap effect is related to some ideal gap in the localized spectral band which is filled due to spinon damping. The resonance peak arises from the itinerant contribution in the presence of superconductivity and vanishes in the normal state. Upon doping, the two contributions show opposite evolution: the intensity of itinerant-hole contribution increases with doping whereas the



localized-spin contribution is reduced as a consequence of the decreasing of the short-range AF correlations. Because of their competition, different types of spin dynamics can be observed as a function of doping. Deeply in the overdoped regime, the localized-spin part becomes negligible which leads to a Fermi-liquid-type picture.

This description appears to be in good agreement with the shape of  $\chi''$  as deduced in our INS experiments. Especially, it gives a consistent physical picture of the spin dynamics in the metallic state of cuprates with doping, from the weakly doped to the heavily doped regime.  $\chi''$  is peaked at the AF wave vector in YBCO, and a continuous shift of its maximum to higher energy is expected on increasing doping<sup>20</sup> as it is clearly observed in INS experiments.<sup>1,10</sup> However, magnetic correlations are still expected at high energies in the heavily doped regime where very small AF intensity is detectable in experiments. Nevertheless, in contrast with most theories, Onufrieva and Rossat-Mignod<sup>20</sup> show that  $\chi''(\mathbf{Q}_{AF}, \hbar\omega)$  has a very low amplitude at high energy as a result of the competition of the two contributions. In the overdoped regime,  $\chi''$  has not yet been calculated in this approach. However, because the localized spin part is reduced upon doping, qualitative agreement with experiments is expected.

### B. Itinerant-hole magnetism picture

Let us now consider a simple itinerant magnetism picture where magnetic fluctuations arise from charge-carrier spin-density fluctuations.<sup>24</sup> This situation, which may occur in cuprates if the hole contribution is strong enough, has been proposed in the weak-coupling limit of the one-band Hubbard model<sup>23</sup> as well as in the infinite- $U$  limit of the  $p$ - $d$  model.<sup>5</sup> In such a case, the noninteracting magnetic susceptibility is described in the normal state as a Lindhard function and is an increasing function of the hole-filling number. Thus, as the doping increases from underdoped to overdoped regime, the itinerant magnetism contribution should be enhanced. However, our experiments have shown, in clear contrast to the itinerant-hole picture, a marked reduction of the weight of  $\chi''$  above  $T_c$  going from YBCO<sub>6.92</sub> to YBCO<sub>7</sub>.<sup>10</sup> Therefore, assuming that the itinerant-hole picture can describe, in some limit, the spin fluctuations in YBCO, the doping dependence of  $\chi''$  indicates that only the overdoped regime can be considered nearby such a possibility. Moreover, to account for the evolution of  $\chi''$  with doping, the short-range AF correlations, the intensity of which obviously decreases with doping, should appear in  $\chi''$  as it is suggested in the strong-coupling limit.<sup>20</sup> The significant reduction in the weight of  $\chi''$  as oxygen is added has been also obtained in the infinite- $U$  limit of the  $p$ - $d$  model<sup>5</sup> when an additional Ruderman-Kittel-Kasuya-Yosida exchange interaction is considered.

In the superconducting state, the itinerant-hole picture predicts that spin fluctuations are suppressed below the superconducting gaps.<sup>5,24</sup> But they are expected at high energy up to an energy scale given by the hole bandwidth. In INS experiments, a high-energy cutoff is observed at much smaller energy than the hole bandwidth value. Moreover, this cutoff is sharper with increasing doping rate, again contrary to what can be expected from usual itinerant magnetism.

Therefore, the itinerant-hole magnetism (Fermi-liquid-type picture) cannot account for the spin dynamics observed in the YBCO system. However, this picture may be valid in the case of strong overdoping. Nevertheless, if we consider that a Fermi-liquid picture applies to the overdoped regime in YBCO, our experimental results show that the magnetic contribution in such a limit is rather weak and hardly significant in INS experiments in the normal state.

### C. INS experiments as a test of the superconducting gap symmetry

Assuming that the spin gap at  $(\pi, \pi)$  wave vector is due to the opening of the superconducting gap,<sup>5,20,23,24</sup> predictions have been made to test the symmetry of the superconducting order parameter.<sup>5,20</sup> In YBCO, a  $q$  scan performed below the spin gap at low temperature should reveal a double-peaked structure at the nodal points  $(2k_F, 2k_F) \approx (0.7\pi, 0.7\pi)$  [i.e.,  $q=0.35$  and  $q=0.65$  in Fig. 1(c)], if the system is indeed a clean  $d$ -wave superconductor. No correlated intensity is sizeable at these nodal points [see Fig. 1(c)] which suggests that the superconducting gap symmetry is not clean  $d$  wave. Such a double structure of a zone diagonal  $q$  scan has never been reported in YBCO. However, these nodal contributions can be very weak compared to the magnetic intensity measured above the gap<sup>20</sup> yielding a nonsizable effect. Therefore, this criterion may be not sufficient to test the  $d_{x^2-y^2}$  superconducting state in absence of any clear positive evidence.

## V. CONCLUSION

To summarize, we have shown that in the overdoped regime of YBCO the magnetic response is restricted over a limited energy range ( $\hbar\omega=33-46$  meV) in the superconducting state. Especially, we have found a spin gap which continues to increase compared to the heavily doped regime. In addition,  $\chi''(\mathbf{Q}_{AF}, \hbar\omega)$  is strongly temperature dependent below  $T_c$ , which can be accounted for by the existence of *two contributions* characterized by two different  $q$  widths. A resonant contribution appears to be strongly connected with superconductivity since it disappears at  $T_c$ . The resonance feature is now reported for  $x>0.9$  by all groups<sup>1,2,7,9,15</sup> between 38 and 41 meV depending either on  $T_c$  or on the *true* oxygen content in each sample. A nonresonant contribution is shown by both the  $q$ , and  $T$  dependences of  $\chi''$ . This part is strongly reduced with increased doping as it can be seen from comparison of  $\chi''$  for different oxygen contents.<sup>10</sup> These AF dynamical correlations are strongly temperature dependent, being nearly suppressed above the superconducting transition. In the normal state, AF fluctuations may be nevertheless sizeable but with an intensity of *one order* of magnitude smaller. Such  $T$  and doping dependences may explain why the second part of  $\chi''$  is not reported by the other groups<sup>2,15</sup> in the overdoped regime. Very recently, the effect of zinc impurities on these AF fluctuations have been emphasized in the superconducting state of fully oxygenated sample.<sup>25</sup> These results clearly show a strong reduction of the resonance feature by substitution of only 2% of zinc ( $T_c=69$  K). Then, the existence of the resonance feature in the superconducting state of YBCO<sub>7</sub> is a key issue for magnetism in cuprates which should be addressed by any theoretical model.

## ACKNOWLEDGMENTS

We are very grateful to Jean Rossat-Mignod who performed a huge work on the topic of this paper. Without his constant determination and his illuminating ideas, most of the properties of magnetic fluctuations in YBCO would be not yet established. We also wish to thank the group of Karlsruhe (K.F.K.) who manages the triple-axis spectrometer

2 T in Saclay: especially W. Reichardt for lending us a large single  $\text{YBa}_2\text{Cu}_3\text{O}_{6.97}$  crystal and M. Braden, N. Pyka, and G. Engel for help and assistance during the experiments. Stimulating discussions with F. Onufrieva, P. Burlet, B. Hennion, M. Lavagna, K. Maki, K. Miyake, C. Pépin, G. Stemman, and H. Won were appreciated. We acknowledge L. Pintschovius and P. Schleger for a critical reading of the manuscript.

- <sup>1</sup>J. Rossat-Mignod, L. P. Regnault, P. Bourges, C. Vettier, P. Burlet, and J. Y. Henry, in *Selected Topics in Superconductivity*, Frontiers in Solid State Sciences Vol 1., edited by L. C. Gupta and M. S. Multani (World Scientific, Singapore, 1993), p. 265; J. Rossat-Mignod, L. P. Regnault, P. Bourges, P. Burlet, C. Vettier, and J. Y. Henry, *Physica B* **192**, 109 (1993).
- <sup>2</sup>H. A. Mook, M. Yethiraj, G. Aeppli, T. E. Mason, and T. Armstrong, *Phys. Rev. Lett.* **70**, 3490 (1993).
- <sup>3</sup>J. M. Tranquada, P. M. Gehring, G. Shirane, S. Shamoto, and M. Sato, *Phys. Rev. B* **46**, 5561 (1992).
- <sup>4</sup>T. E. Mason, G. Aeppli, and H. A. Mook, *Phys. Rev. Lett.* **68**, 1414 (1992); T. R. Thurston, P. M. Gehring, G. Shirane, R. J. Birgeneau, M. A. Kastner, Y. Endoh, M. Matsuda, K. Yamada, H. Kojima, and I. Tanaka, *Phys. Rev. B* **46**, 9128 (1992).
- <sup>5</sup>Q. Si, Y. Zha, K. Levin, and J. P. Lu, *Phys. Rev. B* **47**, 9055 (1993); Y. Zha, K. Levin, and Q. Si, *ibid.* **47**, 9124 (1993); Y. Zha, D. Liu, and K. Levin (unpublished).
- <sup>6</sup>R. Liu, B. W. Veal, A. P. Paulikas, J. W. Downey, P. J. Kostic, S. Fleshler, U. Welp, C. G. Olson, X. Wu, A. J. Arko, and J. J. Joyce, *Phys. Rev. B* **46**, 11 056 (1992).
- <sup>7</sup>J. Rossat-Mignod, L. P. Regnault, C. Vettier, P. Bourges, P. Burlet, J. Bossy, J. Y. Henry, and G. Lapertot, *Physica C* **185–189**, 86 (1991).
- <sup>8</sup>M. Takigawa, A. P. Reyes, P. C. Hammel, J. D. Thomson, R. H. Heffner, Z. Fisk, and K. C. Ott, *Phys. Rev. B* **43**, 247 (1991); M. Horvatic, T. Auler, C. Berthier, Y. Berthier, P. Butaud, W. G. Clark, J. A. Gillet, and P. Segransan, *ibid.* **47**, 3461 (1993).
- <sup>9</sup>J. Rossat-Mignod, L. P. Regnault, P. Bourges, C. Vettier, P. Burlet, and J. Y. Henry, *Phys. Scr. T* **45**, 74 (1992).
- <sup>10</sup>L. P. Regnault, P. Bourges, P. Burlet, J. Y. Henry, J. Rossat-Mignod, Y. Sidis, and C. Vettier, *Physica C* **235–240**, 59, (1994); P. Bourges, L. P. Regnault, J. Y. Henry, C. Vettier, Y. Sidis, and P. Burlet, *Physica B* **215**, 30 (1995).
- <sup>11</sup>L. Pintschovius, *Nucl. Instrum. Methods Phys. Res. Sect. A* **338**, 136 (1994).
- <sup>12</sup>M. Braden, W. Reichardt, and L. Pintschovius (private communication).
- <sup>13</sup>J. D. Jorgensen, B. W. Veal, A. P. Paulikas, L. J. Nowicki, G. W. Crabtree, H. Claus, and W. K. Kwok, *Phys. Rev. B* **41**, 1863 (1990).
- <sup>14</sup>T. Graf, G. Triscone, and J. Muller, *J. Less-Common Met.* **159**, 349 (1990); J. Y. Genoux, T. Graf, A. Junod, D. Sanchez, G. Triscone, and J. Muller, *Physica C* **177**, 315 (1991).
- <sup>15</sup>H. F. Fong, B. Keimer, P. W. Anderson, D. Reznik, F. Dogan, and I. A. Aksay, *Phys. Rev. Lett.* **75**, 316 (1995).
- <sup>16</sup>J. Rossat-Mignod, P. Bourges, F. Onufrieva, L. P. Regnault, J. Y. Henry, P. Burlet, and C. Vettier, *Physica B* **199&200**, 281 (1994).
- <sup>17</sup>M. Sato, S. Shamoto, K. Kiyukura, K. Kakurai, G. Shirane, B. J. Sternlieb, and J. M. Tranquada, *J. Phys. Soc. Jpn.* **62**, 263 (1993).
- <sup>18</sup>P. Bourges, L. P. Regnault, Y. Sidis, and C. Vettier (unpublished).
- <sup>19</sup>See, e.g., V. I. Belinicher and A. L. Chernyshev, *Phys. Rev. B* **47**, 390 (1993); **49**, 9746 (1994).
- <sup>20</sup>F. Onufrieva and J. Rossat-Mignod, *Physica C* **235–240**, 1687 (1994); *Phys. Rev. B* **52**, 7572 (1995).
- <sup>21</sup>F. C. Zhang and T. M. Rice, *Phys. Rev. B* **37**, 3759 (1988).
- <sup>22</sup>T. Tanamoto, H. Kohno, and H. Fukuyama, *J. Phys. Soc. Jpn.* **61**, 1886 (1992); G. Stemmann, C. Pepin, and M. Lavagna, *Phys. Rev. B* **50**, 4075 (1994).
- <sup>23</sup>N. Bulut and D. J. Scalapino, *Phys. Rev. B* **47**, 3419 (1993); M. Lavagna and G. Stemmann, *ibid.* **49**, 4235 (1994); S. V. Maleyev, *J. Phys. (France) I*, **2**, 181 (1992); S. Charfi-Kaddour, R.-J. Tarento, and M. Héritier, *ibid.* **2**, 1853 (1992).
- <sup>24</sup>I. I. Mazin and V. M. Yakovenko, *Phys. Rev. Lett.* **75**, 4134 (1995).
- <sup>25</sup>Y. Sidis, P. Bourges, B. Hennion, L. P. Regnault, R. Villeneuve, G. Collin, and J. F. Marucco, *Phys. Rev. B* (to be published).